Contents lists available at ScienceDirect

# Applied Catalysis B: Environmental

# Sensitivity of supported MoS$_2$-based catalysts to carbon monoxide for selective HDS of FCC gasoline: Effect of nickel or cobalt as promoter

Florian Pelardy [a], Alan Silva dos Santos [a], Antoine Daudin [b], Elodie Devers [b], Thomas Belin [a], Sylvette Brunet [a,*]

[a] Université de Poitiers, Institut de Chimie des Milieux et Matériaux de Poitiers (IC2MP), UMR 7285 CNRS-, 4 rue Michel Brunet, TSA 71106- 86073 Poitiers Cedex 9, France
[b] IFP Energies nouvelles, Rond-point de l'échangeur de Solaize, BP 3, 69360 Solaize, France

A B S T R A C T

The impact of CO, a by-product of biomass transformation, on the transformation of a model FCC gasoline composed of 2-methylthiophene (2MT) and 2,3-dimethylbut-2-ene (23DMB2N) molecules, over MoS$_2$ based catalyst supported over alumina was investigated. More specifically, the effect of the presence and the type of the promoter (Ni or Co) was studied. A gain in activity in HDS of 2MT and hydrogenation of olefins has been confirmed in the presence of the catalysts promoted by cobalt or nickel. However, surprisingly, depending on the promoter (Ni or Co), the effect of the presence of CO is really different. In fact, while the carbon monoxide has a significant negative impact on the CoMoS/Al$_2$O$_3$ catalyst for the transformation of model molecules, no effect is observed for other catalysts. These differences could be attributed to a lower adsorption energy of CO on the non-promoted catalyst and promoted by nickel relative to the catalyst promoted by cobalt as calculated.

© 2017 Elsevier B.V. All rights reserved.

## 1. Introduction

With the spreading of more stringent environmental regulation worldwide on transportation fuels, and particularly to reduce sulfur emissions, hydrodesulfurization processes are always an important for refining market. For example, US and China authorities have now adopted new regulations, that will reduce sulfur content of gasoline fuel below 10 ppm by 2017, as in European Union since 2009 [1–3]. Commercial gasoline is made up of different fractions coming from various refining units: reforming, isomerization and fluid catalytic cracking. FCC gasoline represent 30–50% by volume of the total gasoline pool, but is by far the most important sulfur contributor in gasoline, up to 85–95%. However, it contains also a great quantity of olefins which contributes to a high octane number. Therefore, the challenge is to combine high HDS activity and low olefin hydrogenation. As a consequence, transition metal sulfides catalyst used in this process have to be highly selective (labeled "HDS/HYD"). Indeed, significant olefins saturation can occur during HDS process, leading to a lower octane number.

The molybdenum-based sulfide catalysts supported on alumina have been the subject of numerous studies in the literature for the hydrotreating reactions (hydrodesulfurization, hydrodenitrogenation, hydrodeoxygenation and hydrogenation) [4 and therein, 5,9]. Numerous work on model molecules reported the higher HDS/HYD selectivity of CoMo-type catalysts compare to NiMo ones [4]. These works have conducted catalyst manufacturers to propose CoMo-type catalysts for FCC gasoline HDS processes [5,6] However, the promoting effect of nickel or cobalt could be modified depending on the operating conditions: (temperature, pressure), the presence of H$_2$S and its amount, [6–8]. Thus, previous works on model molecules, have shown that the molybdenum-based catalyst promoted with nickel could be more active than a catalyst promoted with cobalt for the hydrogenation of branched olefins, such as cyclopentene or 3,3-dimethylbut-1-ene, at 150° C and under atmospheric pressure [4,9]. However, these catalysts have similar activity for the hydrodesulfurization of dibenzothiophene, at atmospheric pressure and 400° C [10]. In addition, the catalyst promoted by nickel is much more sensitive to the sulfur content of the feedstock [7–89]. For example, for the transformation of 4,6-dimethyldibenzothiophene under 4 MPa and 340° C depending on the partial pressure of H$_2$S, the NiMoP/Al$_2$O$_3$ and CoMoP/Al$_2$O$_3$ catalysts have different activities [9]. Indeed, the catalyst NiMoP/Al$_2$O$_3$

---

is most active at low partial pressure of $H_2S$. The performance of these two catalysts become similar beyond an $H_2S$ partial pressure of 0.1 MPa. The authors explained these results considering that NiMo catalysts are more sensitive to $H_2S$ than CoMo catalysts since according to the synergy model proposed by Chianelli [11] and the ab initio calculations using the density functional theory [12], the strength of the Mo—S bond would be more reduced after Ni than after Co substitution for Mo at the edges of $MoS_2$ slabs. Then, in a $NiMo/Al_2O_3$ catalyst, sulfur anions would be more basic than those in a $CoMo/Al_2O_3$ catalyst and would be more easily neutralized by the acidic character of $H_2S$.

Furthemore, European Union will impose into petroleum industry to incorporate biofuels with an energetic yield of 10% by 2020 [13]. This means that, in the coming years, the petroleum hydrotreatment process could have to process renewable feedstocks containing oxygenated compounds such as vegetable oils or lignocellulosic biomass since liquids from theses starting materials present a high oxygen content (between 20 and 40%) (containing acid, ester, alcohol functions . . .). Nikulsin et al. [14,15] showed for the co-treating of straight-run diesel fraction and vegetal oil or sunflower oil over Ni(Co)MoS catalysts, a higher activity for the catalyst promoted by Ni than Co. They explained these results by a higher stability of catalyst promoted by Ni than Co. In another way, they concludes that the apparent adsorption constant for triglycerides was 30 times higher on cobalt promoted catalyst than Ni. Consequently, the weak adsorption on Ni promoted catalyst could be related to the different decoration edges than with Co promoted catalyst Very few studies relate the performance of promoted catalysts for hydrodeoxygenation of model oxygenated compounds representative of biooils from lignocellulosic feedstocks [16–,17,18] or hydrodesulfurization of FCC gasoline or gasoil [19–23] in the presence of oxygenates. Whatever the reaction, the presence of carbon monoxide, one of the main by-product of the transformation of biomass feedstock inhibited strongly the HDS reactions over $CoMoS/Al_2O_3$ catalyst. These results were explained by competitive adsorptions on the catalyst surface, CO being the most strongly adsorbed. In other way, an inhibiting effect of CO was also observed on the transformation of 2-ethylphenol (a model molecule representative of liquid from lignocellulosic pyrolysis) over $CoMoS/Al_2O_3$ unlike over $MoS_2/Al_2O_3$ and $NiMoS/Al_2O_3$ catalysts. They explain these results by a competitive adsorption between CO (adsorbed through its carbon atom) and an oxygenated compound on the active sites promoted by Co over both edges, in accordance with DFT studies [24–26] Travert et al. [25] explained the absence of effect of CO on $MoS_2/Al_2O_3$ and $NiMoS/Al_2O_3$ catalysts by a considerably lower adsorption of CO over an unpromoted $MoS_2$ phase or promoted by nickel. This result suggests that the interaction of carbon monoxide with the catalytic surface could be completely different depending on the nature of the transition metal sulfides active phases and could offers perspectives to manage the detrimental effect of CO over CoMo-based catalyst, especially for HDS of FCC gasoline.

Thus, the present paper is a contribution in this direction by studying the effect of CO on the performances of catalysts based on promoted and unpromoted molybdenum based catalyst supported on alumina both in terms of activity and selectivity for the transformation of a model FCC gasoline (composed by 2-methylthiophene and 2,3-dimethylbut-2-ene).

## 2. Experimental part

### 2.1. Catalyst and chemicals

Table 1 reports the characteristic of the molybdenum supported based catalysts provided by IFPEN. These catalysts have been

**Table 1**
Main characteristics of supported molybdenum based oxide catalysts (Pr: Co or Ni promoter).

|  | Pr-O (wt%) | $MoO_3$ (wt%) | Pr/Mo (atom.) | $S_{BET}$ ($m^2$/g) |
|---|---|---|---|---|
| $CoMoS/Al_2O_3$ | 3.0 | 10.0 | 0.58 | 122 |
| $NiMoS/Al_2O_3$ | 2.5 | 12.3 | 0.39 | 116 |
| $MoS_2/Al_2O_3$ | 0 | 10.0 | 0 | 120 |

**Table 2**
Partial pressures (MPa) of the different compounds for the sulfurization step and the transformation of the model FCC gasoline feed (without carbon monoxide).

| Pressure (MPa) | Sulfidation | Model FCC gasoline |
|---|---|---|
| $P_{alkene}$ | 0 | 0.150 |
| $P_{H2S}$ | 0.01 | 0 |
| $P_{2MT}$ | 0 | 0.003 |
| $P_{o-xyl}$ | 0 | 0.190 |
| $P_{H2}$ | 0.09 | 1.31 |
| $P_{nC7}$ | 0 | 0.347 |
| $P_{TOT}$ | 0.1 | 2 |

crushed and sieved to a 250-315 $\mu$m size range and sulfided *in situ* under $H_2S/H_2$ flow (10 mol% $H_2S$) for 10 h at 673 K at atmospheric pressure.

2-methylthiophene (98% purity) has been purchased from Alfa Aesar, 2,3-dimethylbut-2-ene (98% purity) from Acros Organics, o-xylene (>99% purity) from Fluka and *n*-heptane (>99% purity) from Carlo Erba. Chemicals have been used without further purification. Carbon monoxide (1 or 10 vol% in mixture with $H_2$) have been purchased from Air Liquide.

### 2.2. Reaction conditions

Catalytic activity measurements were carried out in a fixed bed reactor at 523 K under a total pressure of 2 MPa with a ratio $H_2$/feed of 360 NL/L.

The model feed FCC gasoline containing 0.3 wt% of 2MT, 20 wt% of 23DMB2N, and 30 wt% of o-xylene (representing aromatics) diluted in n-heptane was injected in the reactor by a HPLC Gilson pump (307 series, pump's head: 5 cm3).

The different partial pressures of the reactants are reported Table 2. O-xylene and n-heptane were not converted under these experimental conditions. The amount of CO added varied from 0 to 0.00131 MPa corresponding to a maximum concentration in hydrogen of 277 ppm.
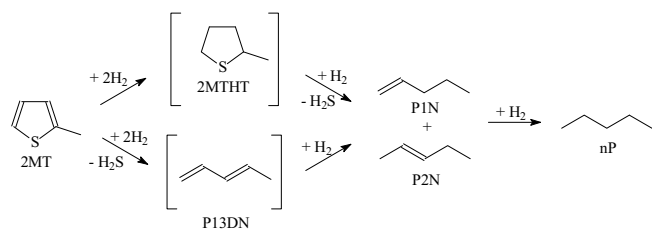
The impact of CO on the transformation of the model feed has been evaluated according to the experimental procedure reported in previous papers [26]:

 (i) transformation of the model feed (up to a conversion close to 30%),
 (ii) mixture of the model feed and CO
 (iii) change of contact time (keeping constant the amount of oxygenated compounds) to reach the reference conversions in order to investigate an eventual modification of the products selectivity,
 (iv) return to the initial conditions used at step (i) in order to investigate the catalyst deactivation and the modification of the selectivity.

The effect of CO alone has been achieved during the same experiment by verifying that the catalyst can be deactivated over time.

### 2.3. Products analysis

The reaction products have been analysed on-line to the fixed bed unit by means of Varian gas chromatograph equipped with

**Scheme 1.** Reaction pathways of the 2-methylthiophene hydrodesulfurization. (2MT: 2-methylthiophene, 2MTHT: 2-methyltetrahydrothiophene, P13DN: pent-1,3-diene, P1N: pent-1-ene, P2N: pent-2-ene, nP: n-pentane).

an automatic sampling valve as described in our previous works [24,27,28]. Desulfurized products, resulting from the transformation of 2-methylthiophene are designated as HDS products. The selectivity of the reaction was calculated by the ratio between hydrodesulfurization (HDS) and olefin hydrogenation (HYD) rate constants, assuming ideal plug flow reactor in gas phase and first order reactions, as defined by Dos Santos et al. [28]. HDS and HYD activities were measured after stabilization of HDS and HYD products formation, respectively and under conditions where a linear relationship between conversion and residence time has been obtained (for a yield in HDS products around 30% and the yield in hydrogenation products around of 30% − all yields and conversions are expressed in molar fraction). The residence time is defined as the ratio between the catalyst weight and the mass liquid feed flow rate. Regarding the transformation of the 2-methylthiophene, HDS products (mainly pentanes and pentenes) are the main observed products according to the reaction scheme described in the literature [29] (Scheme 1). The transformation of the 2,3-dimethylbut-2-ene (23DMB2N) leads to the formation of isomerization products (mainly 2,3-dimethylbut-1-ene, 23DMB1N) and hydrogenation products (mainly 2,3-dimethylbutane, 23DMB) as described previously (Scheme). The double bond isomerization

of 23DMB2N to 23DMB1N is known to be very fast on transition metal sulfides catalysts, compared to HYD reaction so that the mixture composed of 23DMB2N and 23DMB1N is considered as the main reactant [24,27,28,30]. The hydrogenation activity has been measured with the formation of 23DMB which was the main hydrogenation product. Skeletal isomers and their hydrogenated products has been obtained with a yield of less than 1%. To obtain the desired conversion (between 0 and 100%), the residence time has been modified by changing the amount of catalyst used (between 0,075 g and 0,5 g) or the volumic feed flow rate (0.05–8 mL/min). The catalyst activity (±2%) in hydrodesulfurization, corresponding also to the transformation of 2MT, is defined as the number of moles of HDS products formed by hour and by gram of catalyst, and the catalyst activity (±2%) in hydrogenation is defined as the number of moles of 23DMB formed by hour and by gram of catalyst.

### 2.4. XPS analysis

XPS spectra were recorded using a KRATOS AXIS Ultra spectrometer equipped with a (150w) Al Kα monochromatic source (hn = 1486.6 eV). Catalysts were packed in shlenk under argon to avoid sulfate formation. They were identified with reference samples drawn from the Handbook of X-ray photoelectron spectroscopy [30], NIST X-ray Photoelectron Spectroscopy Database (NIST Standard Reference Database 20, Web Version 3.4). The calibration has been made with the carbon peak of contamination identified at 284.6 eV. For each catalyst, the metal and sulfur peaks have been identified according to their binding energies [31,32]. The elemental surface composition of the catalysts, and therefore, the sulfur/metal atomic ratio (S/Me) and the active phase evolution after reaction were determined from the area of the metal and sulfur peaks (the uncertainty of the value is around 20%).
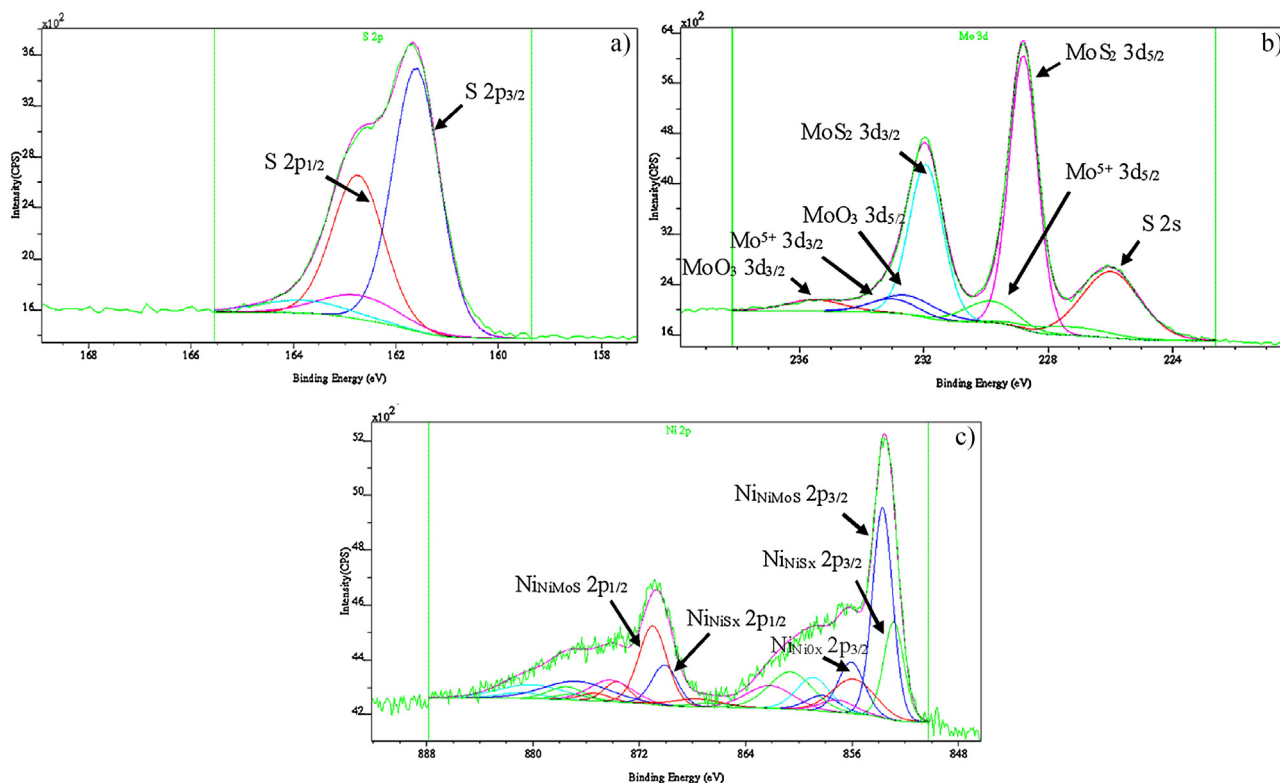


**Fig. 1.** XPS spectra of NiMoS/Al$_2$O$_3$ catalyst after the sulfidation step (a): sulfur element, (b): molybdenum element, (c): nickel element.
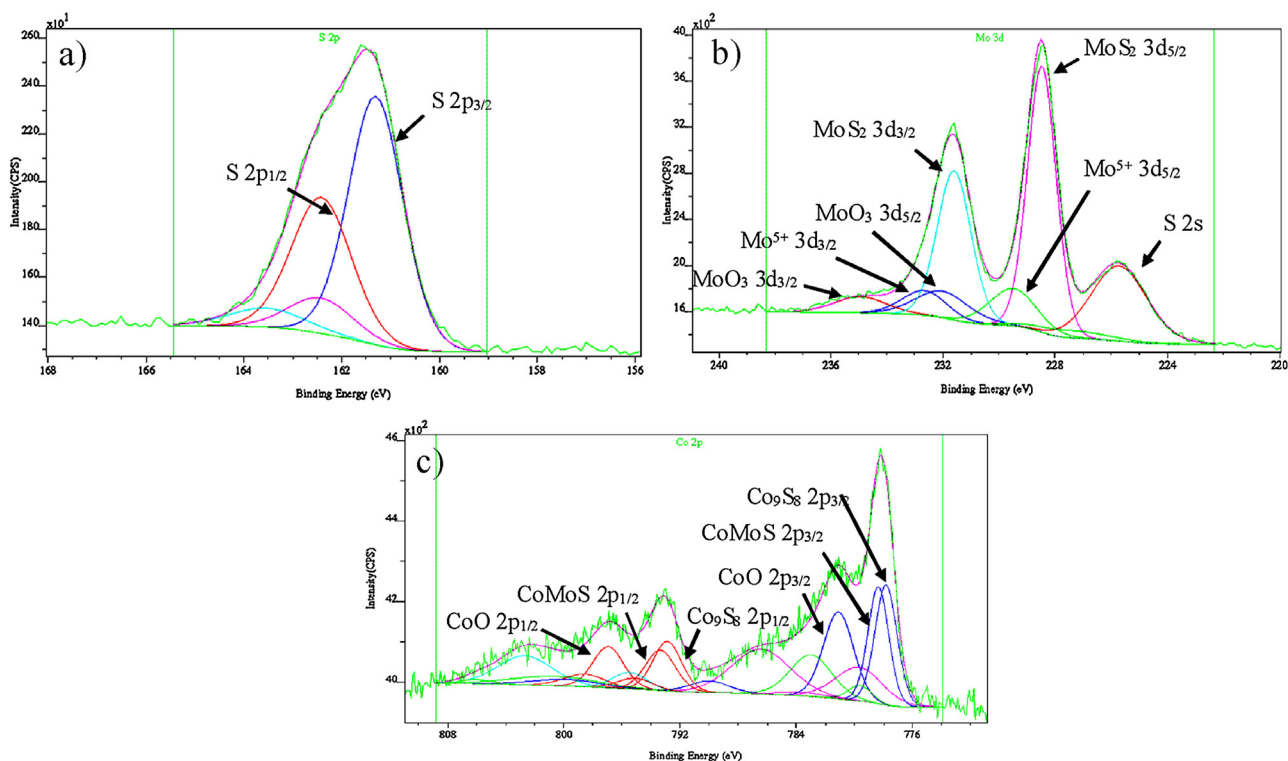
**Fig. 2.** XPS spectra of CoMoS/Al$_2$O$_3$ catalyst after the sulfidation step (a): sulfur element, (b): molybdenum element, (c): cobalt element.

## 3. Results – discussion

### 3.1. Catalyst characterizations

The sulfided molybdenum based catalysts supported on alumina and promoted by nickel or cobalt have been characterized by XPS after the sulfidation step to determine the surface composition. XPS spectra of molybdenum, nickel (or cobalt) and sulfur corresponding to NiMoS/Al$_2$O$_3$, CoMoS/Al$_2$O$_3$ and MoS$_2$/Al$_2$O$_3$ catalysts after sulfidation are shown respectively Fig. 1–3 and Table 3 for the binding energies of the various elements.

Table 4 resumes all of the S/Mo, Co/Mo and Ni/Mo atomic ratios, the promotion by nickel (PNi) or cobalt (PCo), S/Mo atomic ratios, the sulfidation rate of molybdenum (SMo) and the Total sulfidation rate (TS). The S/Mo ratio and the Total sulfidation rate (TS) are constant and respectively equal to 2.1 and around 80% for the tree solids. This clearly demonstrates that the MoS$_2$ phase is well formed in all cases. The introduction of a promoter such as cobalt or nickel has improved the sulfidation rate of molybdenum, since molybdenum sulfidation rate (SM$_O$) are equal to 76 and 78% in the presence of promoter, instead of 68% without promoter. The Co/Mo and Ni/Mo ratios are very close and equal to 0.65. Nevertheless, the promotion by nickel (PNi = 49%) is greater than the promotion by cobalt (PCo = 35%).

### 3.2. Transformation of the model feed over supported molybdenum based catalysts

The transformation of the model feed over the various catalysts (MoS$_2$/Al$_2$O$_3$, NiMoS/Al$_2$O$_3$ and CoMoS/Al$_2$O$_3$) is reported Fig. 4a for the transformation of 2MT and Fig. 4b for the transformation of alkenes. As expected under these conditions, the conversion of 2MT and alkenes were higher with catalysts promoted by nickel or cobalt than supported molybdenum catalyst whatever the residence time. The activity of the NiMoS/Al$_2$O$_3$ catalyst is slightly

higher than CoMoS/Al$_2$O$_3$ (Table 5) for the transformation of 2MT and alkenes (maybe related to the higher active phase content of NiMo catalyst). The transformation of 2MT leads mainly to the formation hydrocarbons C$_5$ (pentenes and pentane) (Fig. 5a). Pentenes (PN) are the primary products which form after a hydrogenation step n- pentane (nP) (Fig. 5b). The formation of n-pentane (nP) is higher over NiMoS/Al$_2$O$_3$ and CoMoS/Al$_2$O$_3$ than MoS$_2$/Al$_2$O$_3$ (Fig. 6a). The yield in cracking products corresponding to the formation of products lower than C$_4$ is not higher than 20% for the higher residence time in the presence of the MoS$_2$/Al$_2$O$_3$ catalyst (Fig. 6b). Whatever the catalyst, the ratio between n-pentane (nP) and pentenes remains constant (Fig. 7). Regarding the hydrogenation of alkenes under HDS operating conditions, the presence of nickel or cobalt reduces the hydrogenation reaction in comparison with the unpromoted sulfided molybdenum supported catalyst (Fig. 8). For example, for a conversion of 80% of 2MT, the hydrogenation yield of alkenes is equal to 49% over MoS$_2$/Al$_2$O$_3$ and only to around 20% over promoted catalysts. However, whatever the catalyst, the hydrogenation yield (HYD) of the alkenes increases strongly with the HDS yield. For example, the HYD yield over MoS$_2$/Al$_2$O$_3$ catalyst rises from 12% to 50% when the HDS yield increases also from 37 to 80%. In the same way, the HYD yield increases from 5 to 48% over CoMoS/Al$_2$O$_3$ and from 4.6 to 41% over NiMoS/Al$_2$O$_3$ when the HDS yield increases from 38 to 99% and from 42 to 96% respectively. As a function of the HDS yield, k$_{HDS}$/k$_{HYD}$ selectivity decreases strongly in the presence of nickel or cobalt. The selectivity factor over promoted catalysts decreases from 9 for CoMoS/Al$_2$O$_3$ and 8 for NiMoS/Al$_2$O$_3$ to 7 when the HDS yield rises from 40 to 100%. At low HDS yield, CoMoS catalysts present higher selectivity than NiMoS catalyst, as reported in the literature, even if, at high conversion the selectivity becomes similar. The selectivity measured over the unpromoted MoS$_2$/Al$_2$O$_3$ catalyst remains lower (k$_{HDS}$/k$_{HYD}$ = 3) and almost stable whatever the HDS yield (Fig. 9).
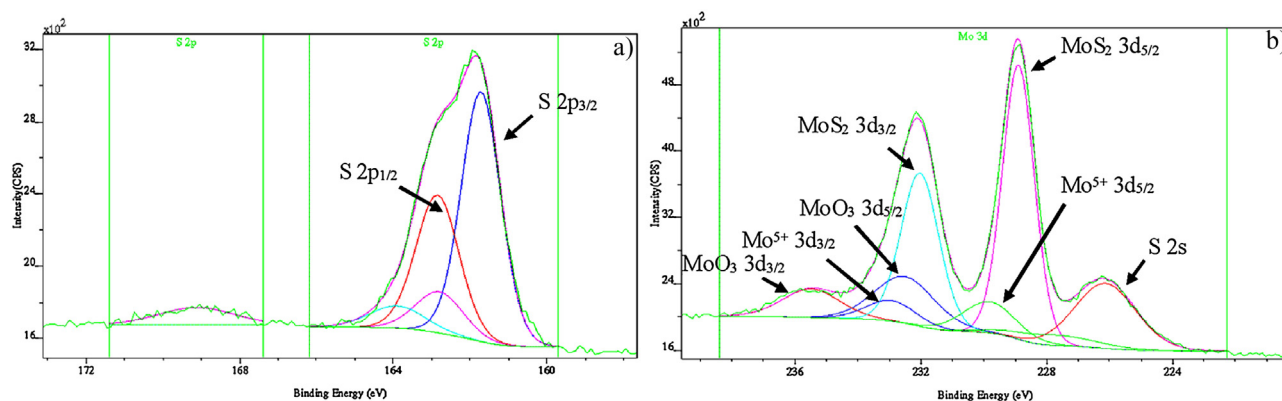
**Fig. 3.** XPS spectra of $MoS_2/Al_2O_3$ catalyst after the sulfidation step (a): sulfur element, (b): molybdenum element.

**Table 3**
XPS characterization of supported molybdenum sulfide based catalysts: binding energies (eV) of the various elements (S $2p_{3/2}$, Mo $3d_{5/2}$, Ni $2p_{3/2}$, Co $2p_{3/2}$).

| | S $2p_{3/2}$ | Mo $3d_{5/2}$ | Ni $2p_{3/2}$ | | | | Co $2p_{3/2}$ | | |
|---|---|---|---|---|---|---|---|---|---|
| | | | NiS | NiMoS | $NiO_x$ | $Co_9S_8$ | CoO | CoMoS |
| $MoS_2$ | 162.2 | 229.4 | – | – | – | – | – | – |
| CoMoS | 162.2 | 229.4 | – | – | – | 778.4 | 781 | 779.1 |
| NiMoS | 162.2 | 229.4 | 852.9 | 853.9 | 856.0 | – | – | – |

**Table 4**
S/Mo, Co/Mo and NiMo atomic ratios, promotion rate by cobalt (PCo%) and by nickel (TNi), sulfidation rate of molydenum (SMo%) and Total sulfidation rate (TS) determined by XPS of $CoMoS/Al_2O_3$, $NiMoS/Al_2O_3$ and $MoS_2/Al_2O_3$ after sulfidation step.

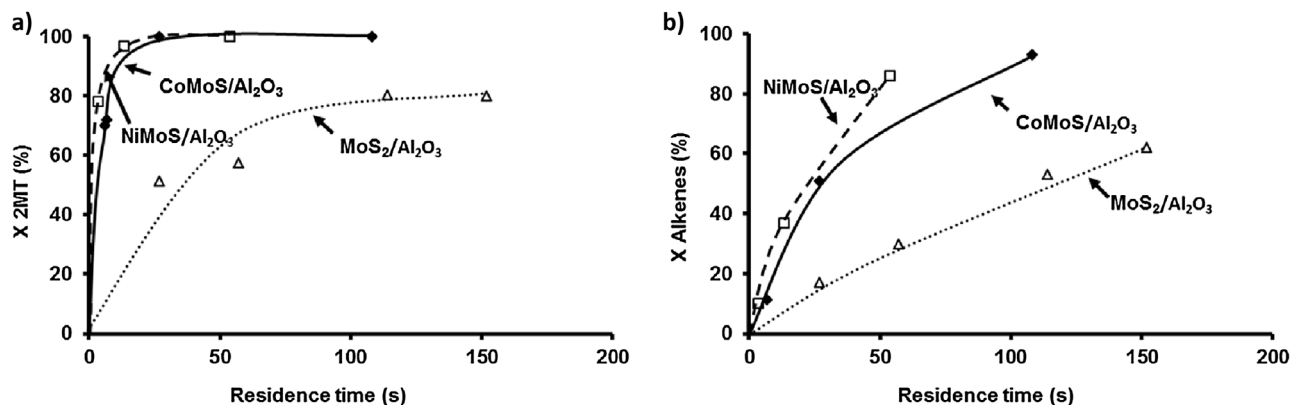| Catalysts | S/Mo | Co/Mo | Ni/Mo | PCo (%) | PNi (%) | SMo (%) | TS (%) |
|---|---|---|---|---|---|---|---|
| $MoS_2/Al_2O_3$ | 2.0 | – | – | – | – | 68 | 75 |
| $CoMoS/Al_2O_3$ | 2.15 | 0.66 | – | 35 | – | 76 | 88 |
| $NiMoS/Al_2O_3$ | 2.0 | – | 0.62 | – | 49 | 78 | 77 |



**Fig. 4.** Transformation of the model feed. Comparison of the performances of $MoS_2/Al_2O_3$, $NiMoS/Al_2O_3$ and $CoMoS/Al_2O_3$ for the conversion of a) 2MT b) alkenes as function of the residence time (T = 250° C, P = 2 MPa, $H_2$/feedstock = 360 NL/L).

**Table 5**
Transformation of the model feed. Comparison of the activity of $MoS_2/Al_2O_3$, $NiMoS/Al_2O_3$ and $CoMoS/Al_2O_3$ catalysts for the transformation of 2MT and alkenes at iso conversion (40% for 2MT and 20% of alkenes) without or with 1.31 MPa of CO. Promoter effect of Ni and Co (in brackets, defined as the activities ratio of promoted catalysts and unpromoted catalyst). (T = 250° C, P = 2 MPa, $H_2$/feedstock = 360 NL/L).

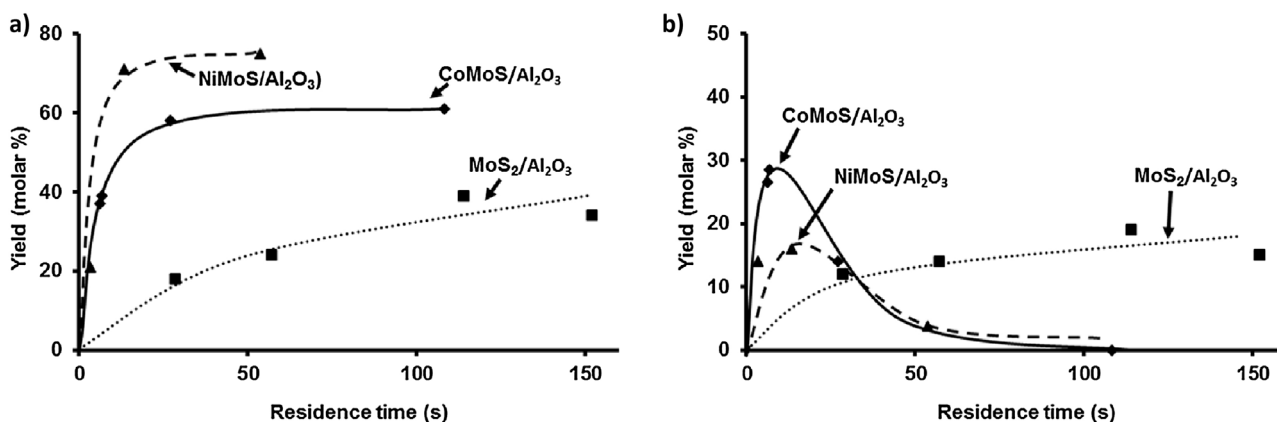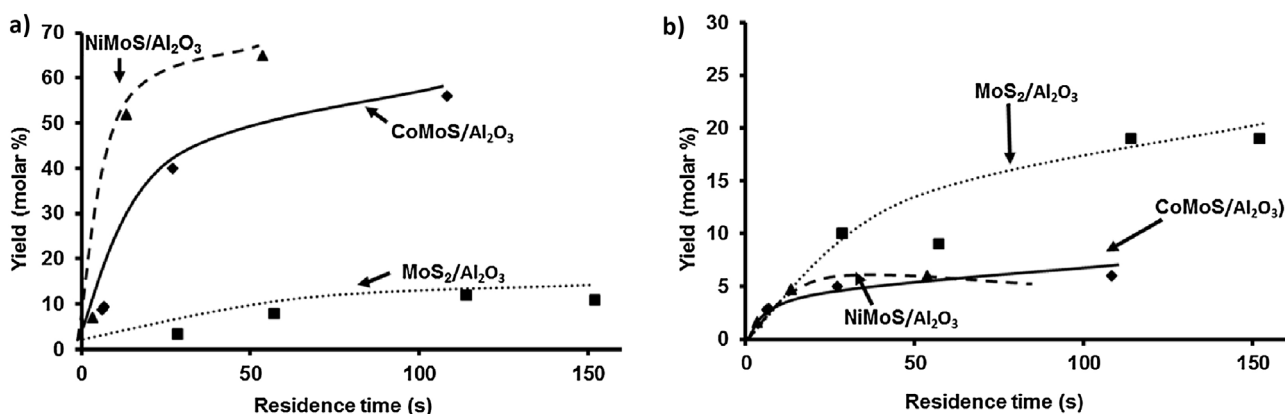| Activity (mmol $h^{-1} g^{-1}$) | 2MT | | Alkenes | |
|---|---|---|---|---|
| | Without CO | With CO | Without CO | With CO |
| $CoMoS/Al_2O_3$ | 1.5(5) | 0.75(2.5) | 1.8(3) | 0.9(1.5) |
| $NiMoS/Al_2O_3$ | 2.3(7.7) | 2.3(7.7) | 2.8(4.7) | 2.6(4.3) |
| $MoS_2/Al_2O_3$ | 0.3(1) | 0.3(1) | 0.6(1) | 0.6(1) |

**Fig. 5.** Transformation of the model feed. Distribution of the products of transformation of 2MT as function of the residence time over $MoS_2/Al_2O_3$, $NiMoS/Al_2O_3$ and $CoMoS/Al_2O_3$ catalysts. a) nC5 (pentenes + pentane) b) pentenes (T = 250° C, P = 2 MPa, $H_2$/feedstock = 360 NL/L).



**Fig. 6.** Transformation of the model feed. Distribution of the products of transformation of 2MT as function of the residence time over $MoS_2/Al_2O_3$, $NiMoS/Al_2O_3$ and $CoMoS/Al_2O_3$ catalysts. a) n-pentane (nP) b) C ≤ 4. (T = 250 °C, P = 2 MPa, $H_2$/feedstock = 360 NL/L).



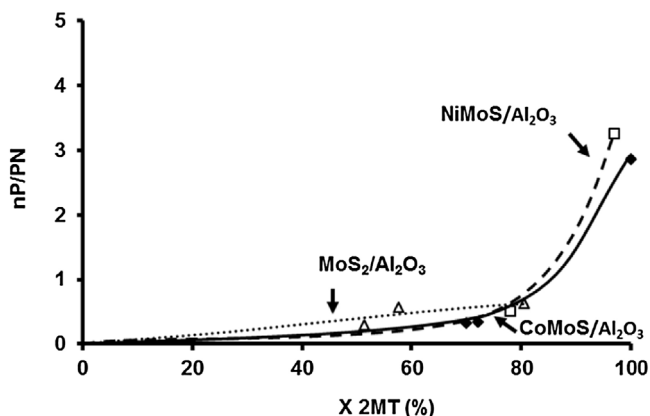**Fig. 7.** Transformation of the model feed. Selectivity nP/PN (n-pentane/pentenes) as function of the conversion over $MoS_2/Al_2O_3$, $NiMoS/Al_2O_3$ and $CoMoS/Al_2O_3$ catalysts. (T = 250 °C, P = 2 MPa, $H_2$/feedstock = 360 NL/L).
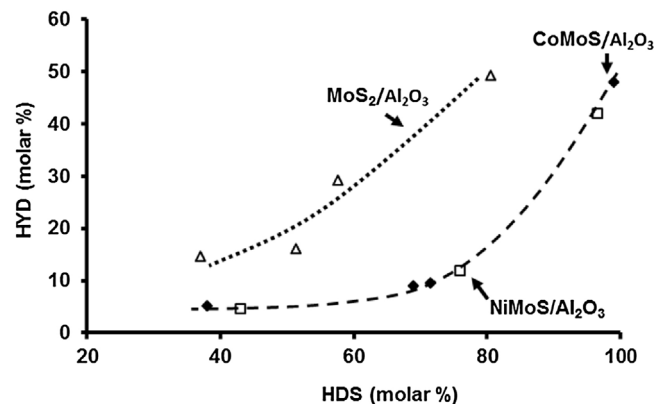
**Fig. 8.** Transformation of the model feed. Change of the hydrogenation of alkenes (HYD) as function of the HDS of 2MT over $MoS_2/Al_2O_3$, $NiMoS/Al_2O_3$ and $CoMoS/Al_2O_3$ catalysts. (T = 250 °C, P = 2 MPa, $H_2$/feedstock = 360 NL/L).

### 3.3. Influence of CO

The impact of the presence of CO with a partial pressure ranging from 0 to 1.31 kPa has been evaluated for the transformation of the model feed over promoted by nickel or cobalt supported sulfided molybdenum catalyst. Under these operating conditions, no transformation of CO was noticed over the three catalytic systems. However, high difference of behavior of these catalytic systems can be noticed by the presence of CO. Indeed, as reported, for

2MT transformation (Fig. 10a) and for the alkenes transformation (Fig. 11a), $NiMoS/Al_2O_3$ remains more active than $CoMoS/Al_2O_3$ and $MoS_2/Al_2O_3$ the less active when CO is introduced and whatever the amount. Nevertheless, $NiMoS/Al_2O_3$ and the unpromoted $MoS_2/Al_2O_3$ did not have the same behavior than $CoMoS/Al_2O_3$ in the presence of CO. Indeed, $NiMoS/Al_2O_3$ and $MoS_2/Al_2O_3$ were almost unsensitive to the presence of CO unlike $CoMoS/Al_2O_3$ catalyst which is dramatically impacted (Figs. 10b, 11b) corresponding to a $A/A_0$ equal to 1 for $NiMoS/Al_2O_3$ and $MoS_2/Al_2O_3$ and to 0.5 for
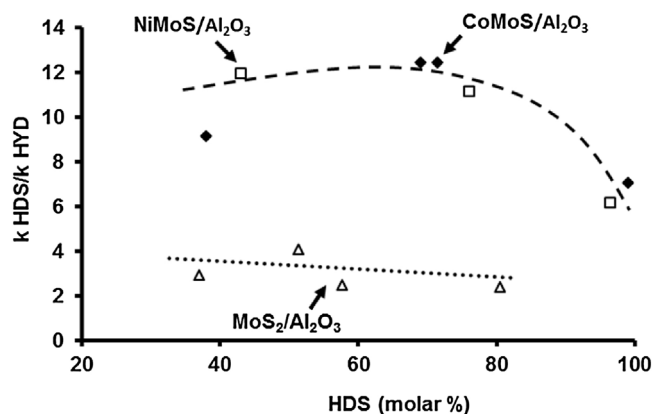
**Fig. 9.** Transformation of the model feed. Selectivity $k_{HDS}/k_{HYD}$ as function of the HDS of 2MT over $MoS_2/Al_2O_3$, $NiMoS/Al_2O_3$ and $CoMoS/Al_2O_3$ catalysts. (T = 250 °C, P = 2 MPa, $H_2$/feedstock = 360 NL/L).

a partial pressure of 1.31 kPa for the $CoMoS/Al_2O_3$ catalyst. This corresponds to a loss of activity of 50% of the initial activity.

Regarding the selectivity measured by the $k_{HDS}/k_{HYD}$, it is relevant to notice no impact of CO for the three catalysts (Table 6).

### 3.4. Kinetic modeling

The experimental results clearly demonstrated a negative impact on CO conversion of the sulfur and olefin molecules in

**Table 6**
Transformation of the model feed. Effect of the partial pressure of CO towards $k_{HDS}/k_{HYD}$ selectivity over $MoS_2/Al_2O_3$, $NiMoS/Al_2O_3$ and $CoMoS/Al_2O_3$ catalysts for the transformation of 2MT and alkenes at iso conversion (40% for 2MT and 20% of alkenes) (T = 250 °C, P = 2 MPa, $H_2$/feedstock = 360 NL/L).

| $P_{CO}$ (kPa) | | 0 | 1.31 |
|---|---|---|---|
| $k_{HDS}/k_{HYD}$ | $CoMoS/Al_2O_3$ | 8.9 | 9 |
| | $NiMoS/Al_2O_3$ | 7 | 6.9 |
| | $MoS_2/Al_2O_3$ | 3.0 | 3.0 |

a mixture. Moreover, this phenomenon is completely reversible since after stopping the injection of the CO, the activity of the catalyst for the transformation of the two model molecules is completely restored. This can be attributed to competition for the adsorption between the various molecules to the surface of the catalyst. In order to determine the adsorption constant of CO on the three catalytic system, a kinetic approach considering the model of Langmuir-Hinshelwood was investigated.

Various hypothesis were made:

1/first order of HDS reaction rate of 2MT and hydrogenation reaction rate of 23DMB2N

2/compounds in the gas phase at the reaction temperature (250 °C)

3/thermodynamic equilibrium between 23DMB2N and 23DMB1N. The reactant involved was 23DMB1N, because it has been shown that it is much more reactive than the 23DMB2N [30].
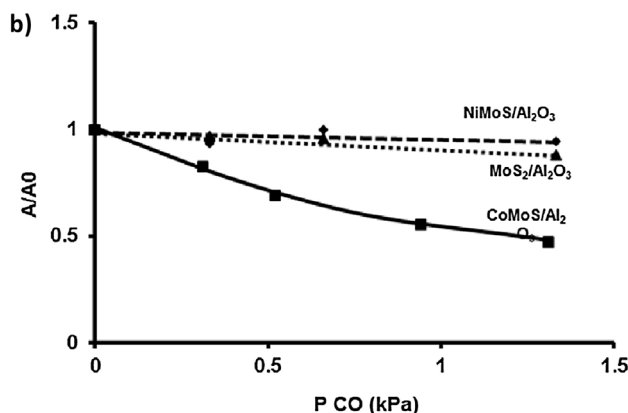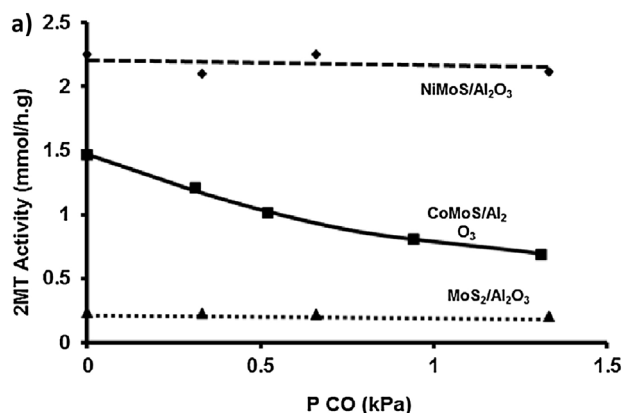


**Fig. 10.** Transformation of the model feed. Effect of the partial pressure of CO on the transformation of 2MT over $MoS_2/Al_2O_3$, $NiMoS/Al_2O_3$ and $CoMoS/Al_2O_3$ catalysts a) Activity b) $A/A_0$ loss of activity (A: activity in the presence of CO, $A_0$: initial activity) over $MoS_2/Al_2O_3$, $NiMoS/Al_2O_3$ and $CoMoS/Al_2O_3$ catalysts. (T = 250 °C, P = 2 MPa, $H_2$/feedstock = 360 NL/L).



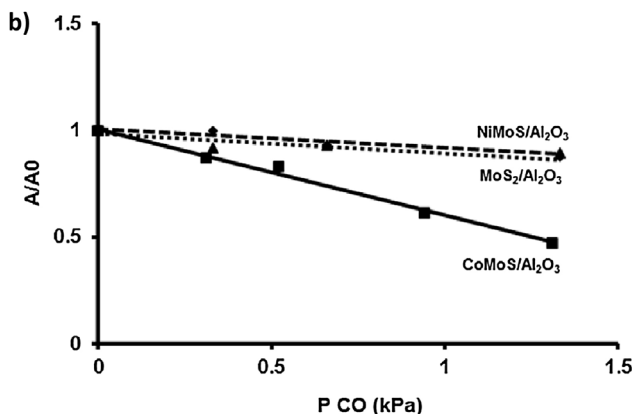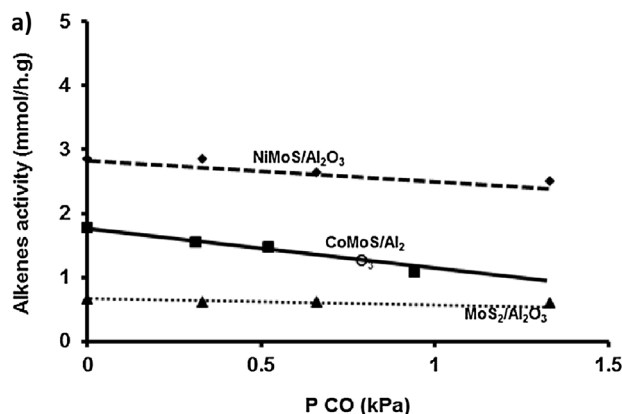**Fig. 11.** Transformation of the model feed. Effect of the partial pressure of CO on the transformation of alkenes over $MoS_2/Al_2O_3$, $NiMoS/Al_2O_3$ and $CoMoS/Al_2O_3$ catalysts a) Activity b) $A/A_0$ loss of activity (A: activity in the presence of CO, $A_0$: initial activity) over $MoS_2/Al_2O_3$, $NiMoS/Al_2O_3$ and $CoMoS/Al_2O_3$ catalysts. (T = 250 °C, P = 2 MPa, $H_2$/feedstock = 360 NL/L).

Moreover, the special operating conditions were taking account:

1/experiments in a large excess of hydrogen

2/2MT partial pressure (3 kPa) very lower than the partial pressure of olefin (150 kPa)

3/partial pressure of olefin constant in the differential domain of the transformation of 2MT

4/CO none converted

To keep the formalism as general as possible, the model proposed in the current work is a one-site model and assumes that $H_2S$ and $H_2$ adsorb dissociatively at the surface, as suggested earlier [29]. The sulfhydryl groups created by $H_2S$ dissociation take part in the elementary steps of the reaction. In what follows, the proposed model for olefin hydrogenation and 2MT hydrodesulfurization reaction. This model considers the HDS reactions of 2MT and hydrogenation of 23DMB1N simultaneously. Thus the reactions involved competitive adsorption of reactants on the same active site and the conservation of the sites is considered.

First, equations (E1) to (E7) describe the basic steps involved in the mechanism for the micro-kinetic model of the hydrogenation of 23DMB1N (noted by R) on a site (M*) (Scheme 2). In agreement with previous work, the determining step is the transfer of the first hydrogen [29]. Similarly, the determining step of the hydrodesulfurization of 2MT (named RS) is the addition of the first hydrogen by MSH. Thus, the hydrogenation step of the thiophene ring prior to the breaking of the C–S bond determines the overall rate of reaction HDS. Steps (E9) to (E19) of this mechanism are reported Scheme 3.

| | | |
|---|---|---|
| $M^* + H_2S \leftrightarrows MS + H_2$ | $K_s$: surface state at the equilibrium | (E1) |
| $MS + M^* + H_2 \leftrightarrows MSH + MH$ | $K_{H2}$: heterolytic adsorption of $H_2$ | (E2) |
| $MS + M^* + H_2S \leftrightarrows 2MSH$ | $K_{H2S}$: heterolytic adsorption of $H_2S$ | (E3) |
| $M^* + R \leftrightarrows MR$ | $K_{23DMB1N}$: Adsorption of 23DMB1N (R) | (E4) |
| $MR + MSH \leftrightarrows MRH + MS$ | $k_{SH}$: Addition of the 1st H by MSH (edv) | (E5) |
| $MRH + MH \leftrightarrows MRH_2 + M^*$ | Addition of 2nd H by MH | (E6) |
| $MRH_2 \leftrightarrows RH_2 + M^*$ | Desorption of hydrocarbon | (E7) |
| $2MSH + H_2 \leftrightarrows 2M^* + 2H_2S$ | surface state at the equilibrium | (E8) |
| $R + H_2 \leftrightarrows RH_2$ | | |

Scheme 2: Elementary steps of the hydrogenation of 23DMB1N.

| | | |
|---|---|---|
| $M^* + H_2S \leftrightarrows MS + H_2$ | $K_s$: surface state at the equilibrium | (E9) |
| $MS + M^* + H_2 \leftrightarrows MSH + MH$ | $K_{H2}$: heterolytic adsorption of $H_2$ | (E10) |
| $MS + M^* + H_2S \leftrightarrows 2MSH$ | $K_{H2S}$: heterolytic adsorption of $H_2S$ | (E11) |
| $M^* + RS \leftrightarrows MRS$ | $K_{2MT}$ 2MT: Adsorption (RS) | (E12) |
| $MRS + MSH \rightarrow MRHS + MS$ | $k_{SH}$: Addition of the 1st H by MSH (edv) | (E13) |
| $MRHS + MH \leftrightarrows MRH_2S + M^*$ | Addition of 2nd H by MH | (E14) |
| $MRH_2S + MH \leftrightarrows MRH_3S + M^*$ | Addition du 3rd H by MH | (E15) |
| $MRH_3S + MH \leftrightarrows MRH_4S + M^*$ | Addition du 4th H by MH | (E16) |
| $MRH_4S + H_2 \leftrightarrows MRH_4 + H_2S$ | Elimination of $H_2S$ | (E17) |
| $MRH_4 + H_2 \leftrightarrows RH_4 + M^*$ | Desorption of the hydrocarbon | (E18) |
| $2MSH + H_2 \leftrightarrows 2M^* + 2H_2S$ | surface state at the equilibrium | (E19) |
| $RS + 3H_2 \leftrightarrows RH_4 + 2H_2S$ | | |

Scheme 3: Elementary steps of the HDS of 2MT

From the elementary steps, the equilibrium constants (K) and concentrations of different species adsorbed ($\alpha$) are expressed by the following equations:

$$K_S = \frac{P_{H_2}}{P_{H_2S}} \cdot \frac{\theta_S}{\theta^*}; K_{H2} = \frac{\theta_{SH}\theta_H}{P_{H2}\theta_S\theta^*}; K_{H2S} = \frac{\theta_{SH}^2}{P_{H2S}\theta_S\theta^*}$$
$$K_{23DMB1N} = \frac{\theta_{23DMB1N}}{P_{23DMB1N}\theta^*}; K_{2MT} = \frac{\theta_{2MT}}{P_{2MT}\theta^*} \tag{1}$$

with: $P_{H2S}$: partial pressure of $H_2S$ $P_{H2}$: partial pressure of hydrogene

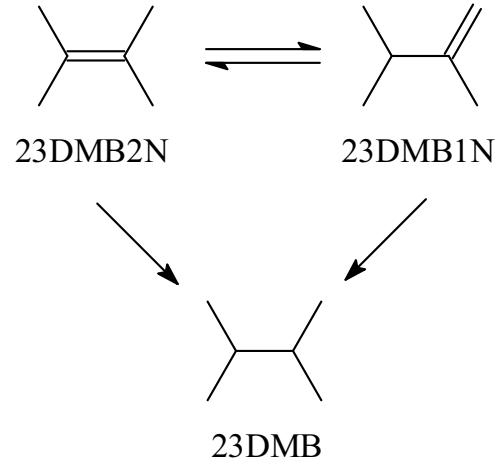$P_{23DMB1N}$: partial pressure of 23DMB1N $P_{2MT}$: partial pressure of 2MT

$\theta^*$: recovery level of the free sites

$\theta_S$: recovery level sites by $H_2S$

$\theta_{SH}$: recovery level sites by sulfhydryl species

$\theta_H$: recovery level sites by hydrogen

$\theta_{23DMB1N}$: recovery level sites by 23DMB1N



**Scheme 2.** Reaction pathways of the 2,3-dimethylbut-2-ene hydrogenation (23DMB2N: 2,3-dimethylbut-2-ene, 23DMB1N: 2,3-dimethylbut-1-ene, 23DMB: 2,3-dimethylbutane).

$\theta_{2MT}$: recovery level sites by 2MT

Whereas the reactions are competitive on the same catalytic sites, the sites conservation equation can be written as:

$$\theta^* + \theta_S + \theta_{SH} + \theta_H + \theta_{23DMB1N} + \theta_{2MT} = 1 \tag{2}$$

Thus, the rate of hydrogenation reactions of 23DMB1N ($r_{HYD}$) and HDS 2MT ($r_{HDS}$) can be written:

$$r_{HYD} = k_{SH(HYD)}\theta_{SH}\theta_{23DMB1N} \tag{3}$$

$$r_{HYD} = k_{SH(HYD)} \frac{\alpha_{23DMB1N}\sqrt{\alpha_{H2S}\alpha_S}}{\left(1 + \alpha_{23DMB1N} + \alpha_{2MT} + \alpha_{H2}\sqrt{\frac{\alpha_S}{\alpha_{H2S}}} + \sqrt{\alpha_{H2S}\alpha_S}\right)^2} \tag{4}$$

and

$$r_{HDS} = k_{SH(HDS)}\theta_{SH}\theta_{2MT} \tag{5}$$

$$r_{HDS} = k_{SH(HDS)} \frac{\alpha_{2MT}\sqrt{\alpha_{H2S}\alpha_S}}{\left(1 + \alpha_{23DMB1N} + \alpha_{2MT} + \alpha_{H2}\sqrt{\frac{\alpha_S}{\alpha_{H2S}}} + \sqrt{\alpha_{H2S}\alpha_S}\right)^2} \tag{6}$$

with

$$\alpha_i = K_iP_i \text{ and } \alpha_S = \frac{P_{H2S}}{K_SP_{H2}} \tag{7}$$

$\alpha_i$: concentration of i species adsorbed

$k$: rate constant

It is therefore possible to develop equations 4 and 6:

$$r_{HYD} = \frac{k_{SH(HYD)}K_{23DMB1N}P_{23DMB1N}\sqrt{K_{H2S}P_{H2S}\frac{P_{H2S}}{K_SP_{H2}}}}{\left(1 + K_{23DMB1N}P_{23DMB1N} + K_{2MT}P_{2MT} + K_{H2}P_{H2}\sqrt{\frac{1}{K_{H2S}K_SP_{H2}}} + \sqrt{\frac{K_{H2S}P_{H2S}^2}{K_SP_{H2}}}\right)^2} \tag{8}$$

$$r_{HDS} = \frac{k_{SH(HDS)}K_{2MT}P_{2MT}\sqrt{K_{H2S}P_{H2S}\frac{P_{H2S}}{K_SP_{H2}}}}{\left(1 + K_{23DMB1N}P_{23DMB1N} + K_{2MT}P_{2MT} + K_{H2}P_{H2}\sqrt{\frac{1}{K_{H2S}K_SP_{H2}}} + \sqrt{\frac{K_{H2S}P_{H2S}^2}{K_SP_{H2}}}\right)^2} \tag{9}$$

To simplify the model kinetic reactions HDS and hydrogenation, approximations are made. It is first possible to consider the partial pressure of H2 to be very high and constant.

Thus the expressions:

$\sqrt{K_{H2S}P_{H2S}\frac{P_{H2S}}{K_S P_{H2}}}$ and $K_{H2}P_{H2}\sqrt{\frac{1}{K_{H2S}K_S P_{H2}}}$ could considered as constant,

and the expression $\sqrt{\frac{K_{H2S}P_{H2S}^2}{K_S P_{H2}}}$ could be negligible compared to 1.

Eqs. (8) and (9) therefore simplify as follows:

$$r_{HYD} = \frac{k'_{SH(HYD)}K_{23DMB1N}P_{23DMB1N}}{\left(1 + K_{23DMB1N}P_{23DMB1N} + K_{2MT}P_{2MT} + K_{H2}P_{H2}\sqrt{\frac{1}{K_{H2S}K_S P_{H2}}}\right)^2} \quad (10)$$

$$r_{HDS} = \frac{k'_{SH(HDS)}K_{2MT}P_{2MT}}{\left(1 + K_{23DMB1N}P_{23DMB1N} + K_{2MT}P_{2MT} + K_{H2}P_{H2}\sqrt{\frac{1}{K_{H2S}K_S P_{H2}}}\right)^2} \quad (11)$$

By taking the square root of the expressions, Eqs. (10) and (11) become:

$$\sqrt{r_{HYD}} = \frac{\sqrt{k'_{SH(HYD)}K_{23DMB1N}P_{23DMB1N}}}{1 + K_{2MT}P_{2MT} + K_{23DMB1N}P_{23DMB1N} + \sqrt{\frac{1}{K_{H2S}K_S P_{H2}}}} \quad (12)$$

$$\sqrt{r_{HDS}} = \frac{\sqrt{k'_{SH(HDS)}K_{2MT}P_{2MT}}}{1 + K_{2MT}P_{2MT} + K_{23DMB1N}P_{23DMB1N} + \sqrt{\frac{1}{K_{H2S}K_S P_{H2}}}} \quad (13)$$

The reactions being of order 1 relative to 23DMB1N and 2MT and that the olefin is transformed slightly in the differential domain of the transformation of 2MT, the following expressions are similar to constants:

$$\frac{\sqrt{k'_{SH(HYD)}K_{23DMB1N}}}{1 + K_{23DMB1N}P_{23DMB1N} + K_{H2}P_{H2}\sqrt{\frac{1}{K_{H2S}K_S P_{H2}}}} = k''_{HYD} \quad (13)$$

$$\frac{\sqrt{k'_{SH(HDS)}K_{2MT}}}{1 + K_{23DMB1N}P_{23DMB1N} + K_{H2}P_{H2}\sqrt{\frac{1}{K_{H2S}K_S P_{H2}}}} = k''_{HDS} \quad (15)$$

Eqs. (14) and (15) can also be written:

$$\sqrt{r_{HYD}} = k''_{HYD}\sqrt{P_{23DMB1N}} \quad (16)$$

$$\sqrt{r_{HDS}} = k''_{HDS}\sqrt{P_{2MT}} \quad (17)$$

and

$$r_{HYD} = k'''_{HYD}P_{23DMB1N} \quad \text{with} \quad k'''_{HYD} = k''^2_{HYD} \quad (18)$$

$$r_{HDS} = k'''_{HDS}P_{2MT} \quad k'''_{HDS} = k''^2_{HDS} \quad (19)$$

The inhibiting effect of CO (without transformation) on the HDS and hydrogenation reactions, by competitive adsorption, can thus be introduced as followed [33,34]:

$$r_{HYD}^{CO} = \frac{k'''_{HYD}P_{23DMB1N}}{1 + K_{CO}^{HYD}P_{CO}} \quad (20)$$

$$r_{HDS}^{CO} = \frac{k'''_{HDS}P_{2MT}}{1 + K_{CO}^{HDS}P_{CO}} \quad (21)$$

and:

$$r_{HYD}^{CO} = k_{HYD}^{CO}P_{23DMB1N} \quad \text{with} \quad k_{HYD}^{CO} = \frac{k'''_{HYD}}{1 + K_{CO}^{HYD}P_{CO}} \quad (22)$$

**Table 7**
Calculated CO adsorption constant $(kPa^{-1})$ over $MoS_2/Al_2O_3$, $NiMoS/Al_2O_3$, $CoMoS/Al_2O_3$ for the transformation of the model feed.

| | $MoS_2/Al_2O_3$ | $NiMoS/Al_2O_3$ | $CoMoS/Al_2O_3$ |
|---|---|---|---|
| 2MT | 0.07 | 0.05 | 0.86 |
| alkenes | 0.09 | 0.09 | 0.68 |

$$r_{HDS}^{CO} = k_{HDS}^{CO}P_{2MT} \quad k_{HDS}^{CO} = \frac{k'''_{HDS}}{1 + K_{CO}^{HDS}P_{CO}} \quad (23)$$

and:

$$\frac{r_{HYD}}{r_{HYD}^{CO}} = 1 + K_{CO}P_{CO} = \frac{k'''_{HYD}}{k_{HYD}^{CO}} \quad (24)$$

$$\frac{r_{HDS}}{r_{HDS}^{CO}} = 1 + K_{CO}P_{CO} = \frac{k'''_{HDS}}{k_{HDS}^{CO}} \quad (25)$$

The determination of the adsorption constant of CO adsorption on the active sites for the hydrogenation and HDS reaction can then be deduced by drawing $\frac{k'''_{HYD}}{k_{HYD}^{CO}} - 1$ as function of the partial pressure of CO

The rate constant ratios may be likened to the ratios of conversions of molecules involved (named Xi with i = 2MT or olefins) and without CO (named $X_0$). From the slopes of the curves (equation 26 and 27), CO adsorption constants for the 2MT transformation (Fig. 12a) and olefins (Fig. 12b) can be calculated and compared for the three catalytic systems ($CoMoS/Al_2O_3$, $NiMoS/Al_2O_3$, $MoS_2/Al_2O_3$). Moreover, Fig. 13a and b respectively for 2MT and olefins transformations show a good correlation between the model and experiments, which confirms the reversible inhibition of CO on the transformation of the model feed (2MT and olefins) according to a Langmuir-Hinshelwood formalism.

The calculated CO adsorption constants are relatively close for 2MT and olefins (Table 7) and reflect the experimental results where a similar effect of CO on the transformation of 2MT and olefins was shown whatever the catalytic systems. In other way, the CO adsorption is higher for $CoMoS/Al_2O_3$ material compared to $NiMoS/Al_2O_3$, and $MoS_2/Al_2O_3$.

## 4. Discussion

The promoting effect of cobalt and nickel was confirmed for the transformation of a model FCC gasoline (composed by 2MT and 23DMB2N). Indeed, the catalysts promoted by nickel and cobalt are more active than the unpromoted catalyst. These results are in agreement with those commonly described in the literature whatever the hydrotreating reactions [4,7]. These results are in good agreement with the fact that Co and Ni are known for weakening the metal–sulfur bond and hence increasing the number of sulfur vacancies considered as active sites (CoMoS and NiMoS mixed sites) [35]. The promoted catalyst by nickel appears more hydrogenating than catalyst promoted by cobalt. The determining factor for the hydrogenation of 23DMB2N is the isomerization 23DMB1N (more reactant for hydrogenation reactions). This step involves the Brønsted acidity of the catalyst. Furthermore, protons of SH groups associated with unsaturated coordination sites (CUS: unsaturated coordinatively sites) adjacent are more acidic in the presence of nickel than in the presence of cobalt. However, under these experimental conditions, the 23DMB2N isomerization into 23DMB1N thermodynamic equilibrium is reached over catalysts based on unpromoted molybdenum. Thus, the isomerization step is not sufficient to explain the differences observed between the hydrogenating activity $NiMoS/Al_2O_3$ catalysts and $CoMoS/Al_2O_3$. This could be explained by a higher rate of promotion in the case of nickel, resulting in the presence of a larger number of active sites.
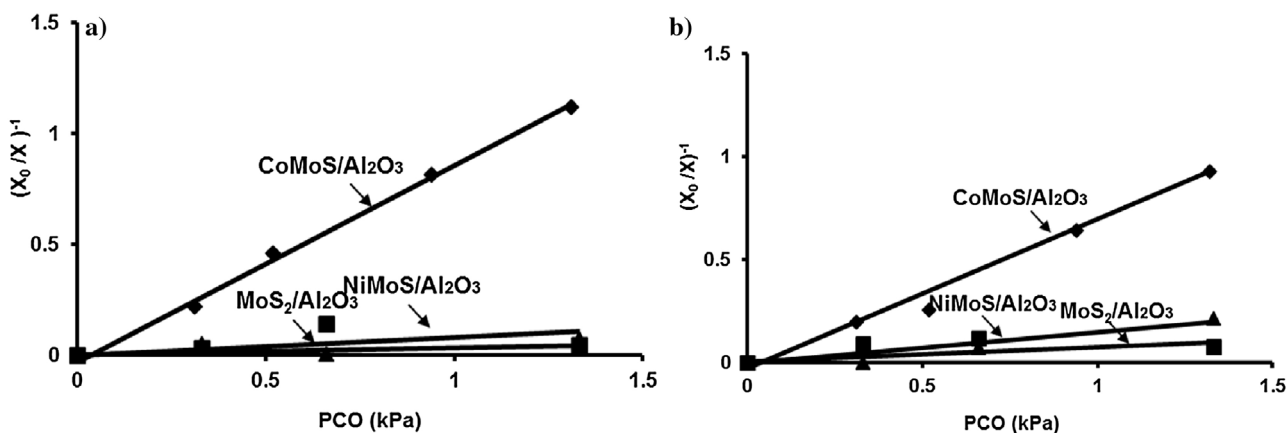
**Fig. 12.** Determination of the adsorption constant of CO over NiMo/Al$_2$O$_3$, CoMo/Al$_2$O$_3$ and Mo/Al$_2$O$_3$. a) 2MT, b) 23DMB1N.
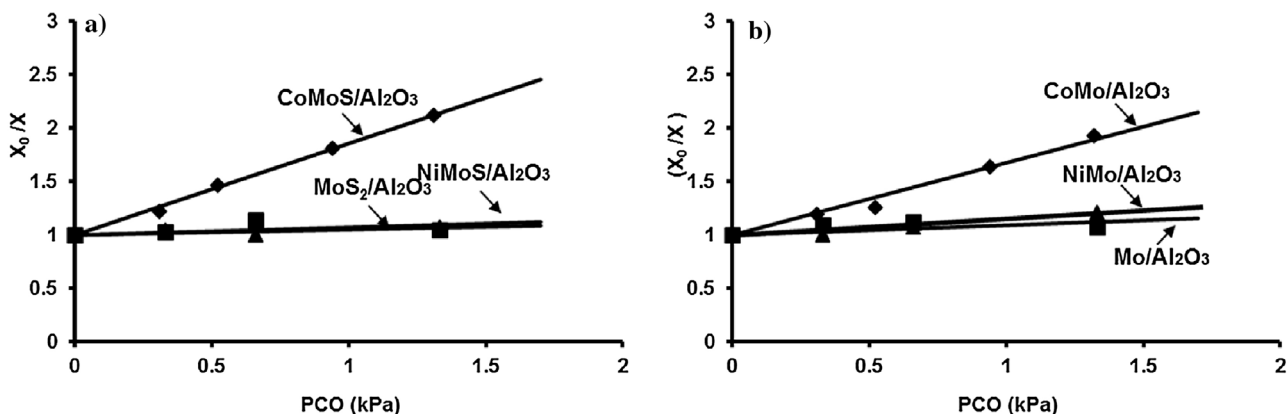


**Fig. 13.** Effect of CO on the transformation of the model feed. Comparison of experiments (points) and model (line). a) 2MT, b) alkenes.

Indeed, by XPS a promotion rate of 49% of molybdenum atom by nickel has been pointed out, against only 35% of cobalt. The difference in activity between the catalyst promoted by nickel or cobalt may also result from increased of the H$_2$ mobility to the catalyst surface, as described in the literature [36].

In the presence of CO, the promoting catalysts remain the most active for the transformation of the model feed. However, these catalysts have a very different behavior from carbon monoxide. While the activity of CoMoS/Al$_2$O$_3$ catalyst is strongly inhibited by the presence of carbon monoxide, surprisingly, the performances of NiMoS/Al$_2$O$_3$ remain almost stable, as unpromoted catalyst. 2MT and olefins transformations (23DMB2N + 23DMB1N) are not changed. As reported in our previous work, the strong inhibiting effect of CO over CoMo catalyst were assumed by competitive adsorption with the sulfur and alkenes compounds, confirmed by DFT calculations where the adsorption energy of CO was higher than the others compounds (H$_2$S, 2MT and 23DMB1N) [24]. This unexpected behavior was rarely reported in the literature due to a lack of data comparison. Similar results were reported by Egeberg et al. [37] on NiMo and CoMo-type catalyst for light gasoil HDS adding carbon monoxide. More recently, Bouvier et al. [19] obtained similar results for the hydrodeoxygenation of 2-ethylphenol as a model compound of bio-crude over sulfided Mo-based catalysts and also by Nikulshin et al. [15,16] for the transformation of sunflower or vegetable oils in co-treatments with straight _run diesel fractions. These results could not be explained by a difference of size of MoS$_2$ slabs which were the same as showed by TEM. In order to explain the difference observed with NiMoS/Al$_2$O$_3$ and MoS$_2$/Al$_2$O$_3$, the different strength of CO adsorption on the surface of these materials as calculated from a kinetic

modeling involving a Langmuir Hinshelwood formalism is considered. One can then speculate that the CO would be much less strongly adsorbed on the NiMoS/Al$_2$O$_3$ and Mo/Al$_2$O$_3$ catalyst surfaces. The catalytic sites would then be much less sensitive to CO. These observations are consistent with the work reported in the literature by Travert et al. [25]. These authors determined by *ab initio* calculations that the CO adsorption energy on a molybdenum-based catalyst was lower if promoted with nickel rather than cobalt and depends also on the degree of promotion and considering M edge and S edge location.

However, there is no result in the literature to supplement our understanding of the lack of inhibitor effect of CO for NiMoS catalyst and unpromoted MoS$_2$ one. From an industrial point of view, our result open a way to optimize catalyst formulation in order to manage CO impact on hydrotreating processes. Future work will be devoted to obtain more detail description of the CO adsorption on NiMoS, CoMoS and MoS$_2$ edge sites to address a better understanding.

## 5. Conclusion

Together, these results confirmed the effect of cobalt and nickel promoter on a molybdenum based catalyst for the transformation of the model charge of a FCC gasoline. Indeed, a gain in activity in HDS 2MT and hydrogenation of olefins has been demonstrated experimentally for the catalysts promoted cobalt or nickel. The NiMoS/Al$_2$O$_3$ catalyst, however, is more active than the catalyst promoted by cobalt. Similarly, a gain of selectivity HDS/HYD is highlighted for promoted catalysts, however, without significant difference in favor of a particular promoter in our operating condi-

tions. These molybdenum-based catalysts promoted with nickel or cobalt present, surprisingly, a very different behavior with respect to CO. Indeed, while the carbon monoxide has a significant negative impact on the CoMoS/Al$_2$O$_3$ catalyst for the transformation of model molecules, no effect is observed for other catalysts. These differences could be attributed to a lower adsorption energy of CO on the non-promoted catalyst and promoted by nickel relative to the catalyst promoted by cobalt, in agreement with theoretical calculations of CO adsorption energies on these materials reported in the literature. Finally, these results show the possibility to optimize the catalyst formulation, especially by modifying the nature of the promoter, depending on the composition of the feed to be treated.

## Acknowledgements

## References

[1] Off. J. Eur. Commun. (2003) (L76/10).
[2] Office of Transportation and Air Quality, US EPA-420-F-14-007, march 2014, http://www.epa.gov/otaq/tier3.htm.
[3] International Coucil on Clean Transportation, China V gasoline and diesel fuel quality standard, regulation GB 17930-2013.
[4] S. Brunet, D. Mey, G. Perot, C. Bouchy, F. Diehl, Appl. Catal. A: Gen. 278 (2005) 143–172.
[5] P. Ghosh, A.T. Andrews, R.J. Quann, T.R. Halbert, Energy Fuels 23 (2009) 5743–5759.
[6] A.-F. Lamic, A. Daudin, S. Brunet, C. Legens, C. Bouchy, E. Devers, Appl. Catal. A: Gen. 344 (2008) 198–204.
[7] C. Fontaine, Y. Romero, A. Daudin, E. Devers, C. Bouchy, S. Brunet, Appl. Catal. A: Gen. 388 (2010) 188–195.
[8] V. Rabarihoela-Rakotovao, S. Brunet, G. Perot, F. Diehl, Appl. Catal. A: Gen. 306 (2006) 34–44.
[9] M. Badawi, L. Vivier, G. Pérot, D. Duprez, J. Mol. Catal. A: Chem. 293 (2008) 53–59.
[10] J. Mijoin, V. Thévenin, N. Garcia Aguirre, H. Yuze, J. Wang, W.Z. Li, G. Pérot, J.L. Lemberton, Appl. Catal. A: Gen. 180 (1999) 95–103.
[11] R.R. Chianelli, Catal. Rev. Sci Eng. 26 (1984) 361.
[12] R.R. Chianelli, G. Berhault, P. Raybaud, S. Kasztelan, J. Hafner, H. Toulhoat, Appl. Catal. A: Gen. 227 (2002) 83.
[13] Directive 2009/30/CE L140/88.
[14] A.N. Varakin, V.A. Salnikov, M.S. Nikulshina, K.I. Maslakov, A.V. Mozhaev, P.A. Nikulshin, Catal. Today (2016) (in press).
[15] P.A. Nikulshin, V.A. Sal'nikov, Al A. Pimerzin, Yu V. Eremina, A.S. Koklyukhin, V.S. Tsvetkov, A.A. Pimerzin, Pet. Chem. 56 (1) (2016) 56–61.
[16] S. Brillouet, E. Baltag, S. Brunet, F. Richard, Appl. Catal. B: Environ. 148–149 (2014) 201–211.
[17] Y. Romero, F. Richard, Y. Reneme, S. Brunet, Appl. Catal. A: Gen. 353 (2009) 46–53.
[18] C. Bouvier, Y. Romero, F. Richard, S. Brunet, Green Chem. 13 (2011) 2441–2451.
[19] A. Pinheiro, D. Hudebine, N. Dupassieux, C. Geantet, Energy Fuels 25 (2011) 804–812.
[20] M. Philippe, F. Richard, D. Hudebine, S. Brunet, Appl. Catal. A Gen. 383 (2010) 14–23.
[21] A. Pinheiro, D. Hudebine, N. Dupassieux, C. Geantet, Energy Fuels 25 (2011) 804–812.
[22] F. M.Philippe, D. Richard, S. Hudebine, Appl. Brunet, B. Catal, Environmental 132–133 (2013) 493–498.
[23] F. Pelardy, C. Dupont, C. Fontaine, E. Devers, A. Daudin, F. Bertoncini, P. Raybaud, S. Brunet, Appl. Catal. B: Environ. 97 (2010) 323–332.
[24] A. Travert, C. Dujardin, F. Mauge, E. Veilly, S. Cristol, J.-F. Paul, E. Payen, J. Phys. Chem. B 110 (2006) 1261–7095.
[25] M. Badawi, J.-F. Paul, S. Cristol, E. Payen, Catal. Commun. 12 (2011) 901–903.
[26] F. Pelardy, C. Dupont, E. Devers, A. Daudin, P. Raybaud, S. Brunet, Appl. Catal. B: Environ. 183 (2016) 1–11.
[27] A. Daudin, S. Brunet, G. Pérot, P. Raybaud, C. Bouchy, J. Catal. 248 (2007) 111–119.
[28] N. Dos Santos, H. Dulot, N. Marchal, M. Vrinat, Appl Catal A: Gen. 352 (2009) 114–123.
[29] D. Mey, S. Brunet, C. Canaff, G. Pérot, C. Bouchy, F. Diehl, F. Maugé, J. Catal. 227 (2004) 436–447.
[30] C.D. Wagner, W.M. Riggs, L.E. Davis, J.F. Moulder, in: G.E. Muilenberg (Ed.), Handbook of X-ray Photoelectron Spectroscopy, Perkin-Elmer Corporation (PhysicalElectronics), 1979.
[31] A.D. Gandubert, C. Legens, D. Guillaume, S. Rebours, E. Payen, Oil Gas Sci. Technol. Rev. IFP 62 (2007) 79–87.
[32] K. Marchand, C. Legens, D. Guillaume, P. Raybaud, Oil Gas Sci. Technol. Rev. IFP 64 (6) (2009) 719–730.
[33] L.C. Gutberlet, R.J. Bertolacini, Ind. Eng. Chem. Prod. Res. Dev. 22 (1983) 246–254.
[34] E. Laurent, B. Delmon, Ind. Eng. Chem. Res. 32 (1993) 2516–2524.
[35] P. Raybaud, Appl. Catal. A 322 (2007) 76–91.
[36] S. Blanchin, P. Galtier, S. Kasztelan, S. Kressmann, H. Penet, G. Perot, J. Phys. Chem. 105 (2001) 10860–10866.
[37] R.G. Egeberg, N. H. Egebjerg, S. Nystrom, NPRA Annual Meeting, 2010 Turning over a new leaf in renewable diesel hydrotreating.